

Multi-Inductor Multi-Output Hybrid (MiMoH) Converter for Large Conversion Ratio and Multiple Outputs

Ratul Das and Hanh-Phuc Le

Department of Electrical and Computer Engineering, University of California San Diego
La Jolla, California, USA
{ratuldas, hanhphuc}@ucsd.edu

Abstract—In this paper, a new multi-inductor multi-output hybrid (MiMoH) converter is proposed and demonstrated. The structure is synthesized from the popular series capacitor Buck (SCB) converter to provide multiple output voltages. The relationship between voltages and the power of the outputs is analyzed to provide output regulation with duty cycle modulation. A MiMoH converter prototype has been implemented to demonstrate conversion from a 24-48V input voltage to three individually regulated outputs ranging from 1.2V to 2.2V. The converter prototype achieves 40W peak power and 91.8% peak efficiency.

Index Terms—Multi output, DC-DC, Switched capacitor, Hybrid

I. INTRODUCTION

Each modern electronic appliances is a set of individual smaller electronic systems dedicated to more specific tasks. These smaller systems complement and coordinate with each other to finally serve the purpose of the whole system. In most cases, the whole system is powered by a single voltage source, while the smaller parts use different voltage rails for their operation. Modern televisions, mobiles, computers, etc., are examples of different power rails for processors, displays, memory, communication devices, and other individual functional blocks. Even within a processor chip, computation demands have driven the design to have multiple cores that require different voltage levels (in dynamic voltage and frequency scaling, or DVFS) and power to achieve optimal energy per computation efficiency.

To support these multiple voltage rails, the system power delivery often starts from a higher voltage level and uses either multiple high-voltage (HV) high conversion ratio converters or multiple stages comprised of a single HV converter followed by multiple low-voltage (LV) Buck converters. These solutions suffer from a deficiency in area utilization or low efficiency from the series connection of multiple stages. Therefore, it is desirable to seek a new converter architecture that can deliver high conversion ratios while providing multiple outputs in a single converter stage. In literature, multi-output

converters use transformers with multiple secondary windings for multiple outputs [1] or single inductor multiple output (SIMO) architectures with minimal voltage conversion capability [2]–[4]. In this work, we propose a switched capacitor-based hybrid converter to operate at a high conversion ratio and provide simultaneous multiple outputs. Section II describes the converter with its operation, and section III follows with the steady-state analysis. The converter hardware implementation and experimental verification are included in Section IV. The paper is summarized and concluded in Section V.

II. PROPOSED MiMoH CONVERTER

Historically, Series Capacitor Buck (SCB) converter shown in Fig. 1a was proposed and demonstrated in [5], although the popular customary name was given in a later publication [6]. The same topology was also synthesized from the switched capacitor-based converter's perspective later in [7]–[10]. Following the synthesis of the series capacitor Buck converter from a Dual inductor hybrid converter in [11], recent high current demonstrations for data center applications have been done with the favorable modification of the SCB converter [12]–[14]. The inductors in the SCB converter serve one output. However, we recognize that these inductors can be separated to provide multiple individual outputs,

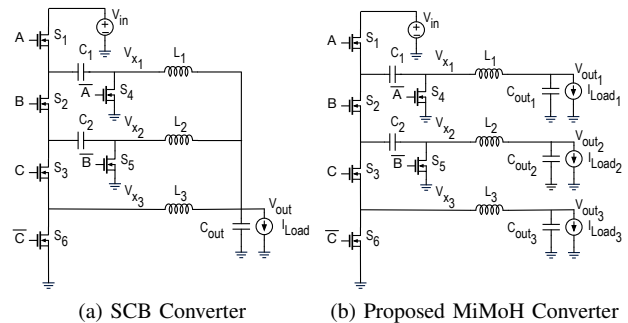


Figure 1: Synthesis of the new topology

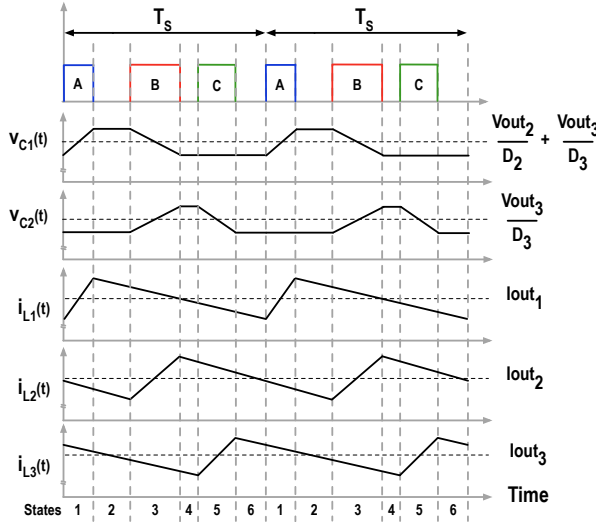


Figure 2: Timing diagram

thus constructing the multi-inductor multi-output hybrid (MiMoH) converter. There can be multiple variations of MiMoH converter in terms of the number of levels, capacitors and their connections, inductors, and outputs [15]. However, in this work, we focus on the 3-level 3-inductor 3-output converter, shown in Fig. 1b, that can carry the essence of the MiMoH converter.

The proposed MiMoH converter has two flying capacitors C_{1-2} , three inductors L_{1-3} , and three pairs of switches ($S_{1,4}$, $S_{2,5}$, and $S_{3,6}$) working at three different phases A, B and C. Two complementary signals control two switches in a pair. The operation of the converter can be explained with the timing diagram in Fig. 2 and the converter states in Fig. 3. Three operating phases divide the switching period into six different converter states. In state 1 (Fig. 3a) when switch S_1 is on, inductor L_1 softly charges capacitor C_1 while also supplying the load at V_{OUT_1} . Similarly in state 3 (Fig. 3b), inductor L_2 discharges C_1 , charges C_2 , and supplies V_{OUT_2} . Then, inductor L_3 discharges C_2 to supply V_{OUT_3} in state 5. While in states 1, 3, and 5, one inductor

current is charged, and the other two are discharged in freewheeling; all three inductors freewheel in states 2, 4, and 6. For normal operation, the non-overlapped operation needs to be maintained between states 1 and 3 and between states 3 and 5. The operating phases A, B, and C, corresponding to states 1, 3, and 5, can be arranged in any order or phase shifts as long as the non-overlap condition is satisfied. As three inductors serve the three outputs separately, the outputs can be regulated by the time the inductors get charged and thus, changing the slopes of the inductor currents.

III. STEADY STATE ANALYSIS

Assume the duty cycles of the phases A, B, and C are D_1 , D_2 , and D_3 , respectively and voltages of capacitors C_{1-2} are $V_{C_{1-2}}$. Applying the volt-second balance to the inductors, we can get the following relationships among input, output, and flying capacitor voltages:

$$V_{in} = \frac{V_{out_1}}{D_1} + \frac{V_{out_2}}{D_2} + \frac{V_{out_3}}{D_3}, \quad (1)$$

$$V_{C_1} = \frac{V_{out_2}}{D_2} + \frac{V_{out_3}}{D_3}, \text{ and } V_{C_2} = \frac{V_{out_3}}{D_3}$$

However, (1) does not provide information on how to regulate each output voltage individually. Thus, this converter breaks the norms of traditional pulse-width modulated (PWM) converters such as Buck, Boost, or even the parent SCB converter, [5], [10] where the duty cycle can be directly calculated by deriving the input to output conversion ratio from the volt-second balance. So, we need to look into other fundamental relationships.

Other ways to analyze a power converter are to use charge balance and/or power balance. In a switched capacitor-based converter, the same charge normally flows from one flying capacitor to another. This charge is directly linked to the output current. In the proposed MiMoH converter, the inductors can carry different currents to support their respective outputs, or $I_{L_i} = I_{out_i}$. These currents charge and discharge flying capacitors C_{1-2} during states 1, 3, and 5. For simplicity in analysis,

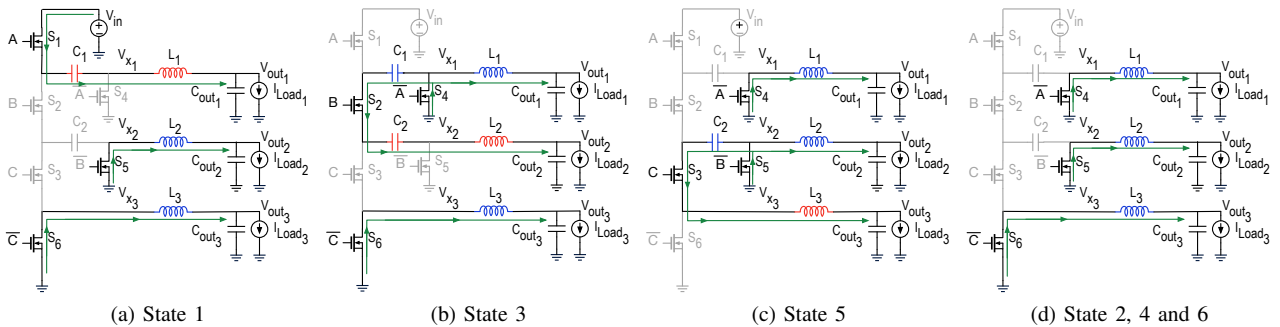


Figure 3: Operating states of the proposed MiMoH converter

second-order effects from the L-C interaction listed in [16] are considered insignificant. Thus, the inductor currents are assumed to charge and discharge with constant slopes. Hence, applying the charge balance on C_{1-2} , we get the following relationship:

$$I_{out_1}D_1 = I_{out_2}D_2 = I_{out_3}D_3 \quad (2)$$

We can also write the theoretical power balance equation in the converter and apply (2):

$$P_{in} = P_{out} = P_{out_1} + P_{out_2} + P_{out_3} \quad (3)$$

$$\begin{aligned} V_{in}I_{in} &= V_{in}I_{out_1}D_1 \\ &= V_{in}I_{out_2}D_2 = V_{in}I_{out_3}D_3 \quad (4) \\ &= V_{out_1}I_{out_1} + V_{out_2}I_{out_2} + V_{out_3}I_{out_3} \end{aligned}$$

From (4), the duty cycles for the three phases can be calculated to have relationships with different voltages, currents and power for different outputs as follow:

$$\begin{aligned} D_1 &= \frac{V_{out_1}}{V_{in}} + \frac{V_{out_2}}{V_{in}} \frac{I_{out_2}}{I_{out_1}} + \frac{V_{out_3}}{V_{in}} \frac{I_{out_3}}{I_{out_1}} \\ &= \frac{V_{out_1}P_{out}}{V_{in}P_{out_1}} \end{aligned} \quad (5)$$

$$\begin{aligned} D_2 &= \frac{V_{out_1}}{V_{in}} \frac{I_{out_1}}{I_{out_2}} + \frac{V_{out_2}}{V_{in}} + \frac{V_{out_3}}{V_{in}} \frac{I_{out_3}}{I_{out_2}} \\ &= \frac{V_{out_2}P_{out}}{V_{in}P_{out_2}} \end{aligned} \quad (6)$$

$$\begin{aligned} D_3 &= \frac{V_{out_1}}{V_{in}} \frac{I_{out_1}}{I_{out_3}} + \frac{V_{out_2}}{V_{in}} \frac{I_{out_2}}{I_{out_3}} + \frac{V_{out_3}}{V_{in}} \\ &= \frac{V_{out_3}P_{out}}{V_{in}P_{out_3}} \end{aligned} \quad (7)$$

In a voltage converter, the most important feature would be regulating the right output voltage(s). As

shown in (5)-(7), controlling the duty cycle to regulate an output voltage in the MiMoH converter depends on the power requirement of other outputs. This behavior has an impact on the flying capacitor voltages. At the converter switching frequency, flying capacitors can be considered voltage sources. While the input is the power source for all three outputs, capacitor C_1 acts as an intermediate power source for V_{out_2} and V_{out_3} , and capacitor C_2 as an intermediate power source for V_{out_3} . As the input voltage is constant, the flying capacitor voltages need to move around to accommodate the power increase or decrease in different outputs. This behavior of the flying capacitor voltages can be modeled by modifying the equations of (1) using (5)-(7) as follows:

$$\begin{aligned} V_{C_1} &= \frac{V_{in}(P_{out_2} + P_{out_3})}{P_{out}}, \text{ and} \\ V_{C_2} &= \frac{V_{in}P_{out_3}}{P_{out}} \end{aligned} \quad (8)$$

Note that the flying capacitor voltages in the MiMoH converter are fully predictable based on (8), and do not suffer from the known balancing issue of 3-level Buck converter [16], [17].

IV. EXPERIMENT RESULTS

A proof-of-concept prototype of the converter, shown in Fig. 4, was built using the components listed in Table I. GaN devices have been used to implement all the power switches in the converter. The cascaded bootstrap technique is applied to power gate driving circuits [18]. The measured waveforms of the converter are shown in Figs. 5a and 5b, proving its intended stable operation. These waveforms are taken at 24V to simultaneous three regulated output operations at 1.5V/5A, 1.8V/5A, and 1.2V/5A. It can be seen from Fig. 5b that the flying capacitors are softly charged and discharged by the inductors. The switching node voltages $V_{x_{1-3}}$ have different swings as they support different output voltages. $V_{x_{1-3}}$ levels can be calculated from the flying capacitor voltages in 8. The inductor currents are at the same DC levels as the output currents.

There can be numerous settings of output voltages and power that the MiMoH converter can support. In this paper, we include measured performances of the converter in several example combinations for output

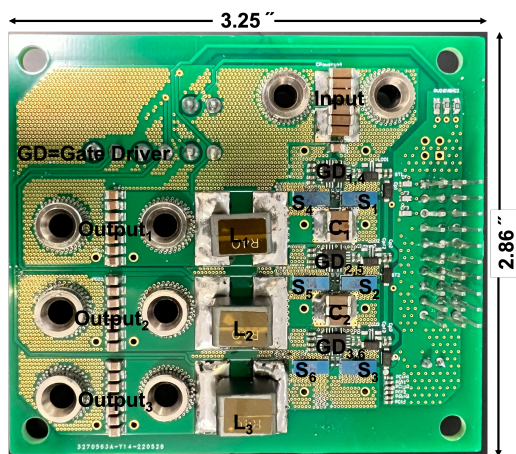
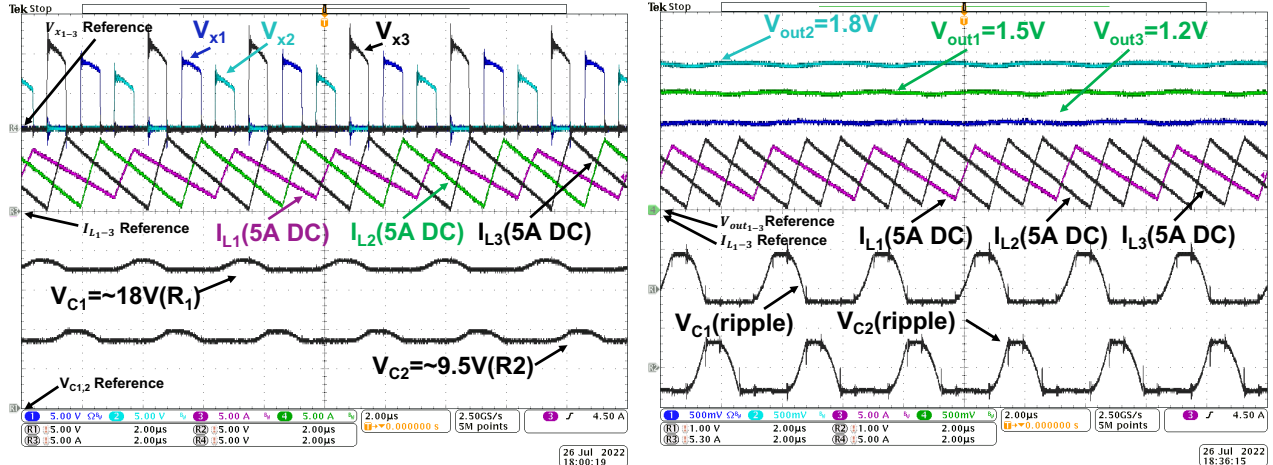


Figure 4: Prototype of the converter

Table I: Components used in MiMoH converter

Components	Part Number
Sw ₁₋₃	60V EPC2020
Sw ₄₋₆	30V 2xEPC2023
C ₁₋₅	2x1.4uF 50V C1812C145J5JLC7805
L ₁₋₃	400nH VLBU1007090T-R40L
Gate Driver	LMG1210



(a) Switching node voltages and inductor currents with DC coupled flying capacitor voltages

(b) Output voltages and inductor currents with AC coupled flying capacitor voltages

Figure 5: Measured waveforms at 24V to simultaneous 1.2V/5A, 1.5V/5A, and 1.8V/5A operation

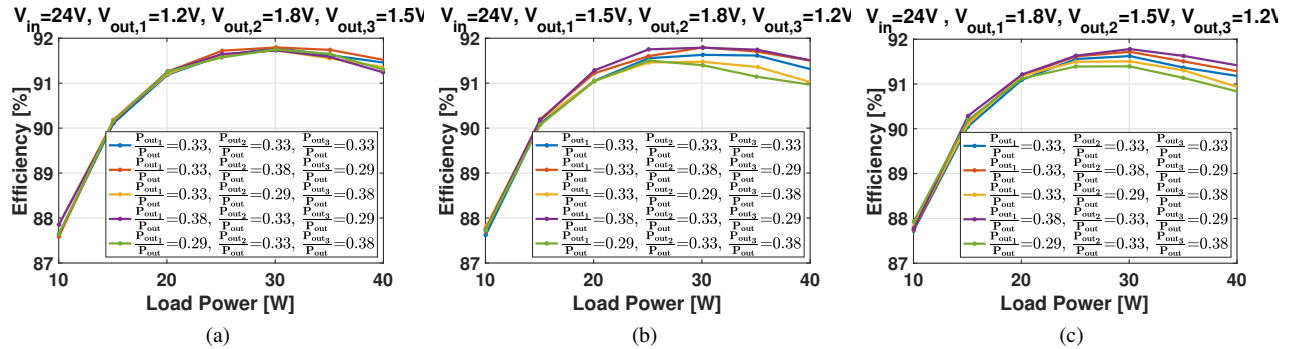


Figure 6: Performance of the converter at 24V input

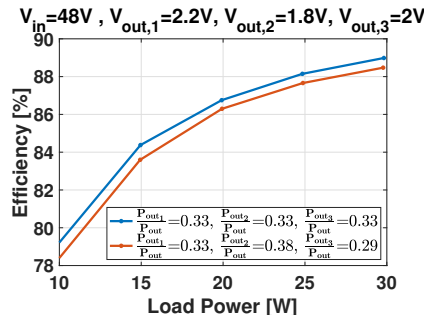


Figure 7: Performance of the converter at 48V input

voltages from 1.2V to 2.2V in Fig. 6 and 7. Figures 6a-6c show the performance of the converter with different combinations of output voltages 1.2V, 1.5V, and 1.8V from an input voltage of 24V, achieving a peak efficiency of 91.8%. Figure 7 shows the efficiency measurement at 48V input voltage and 2.2V, 1.8V, and 2V output voltages. In this operating condition, the converter

achieves 88.9% efficiency. The peak power delivered by this converter in this set of measurements is 40W.

During all these measurements, a control loop was employed to robustly regulate output voltages in an automated manner for all the conditions of output current, voltage, and power levels. This control loop was designed based on equations (5)-(7).

V. CONCLUSION

A high conversion ratio multi-inductor multi-output hybrid (MiMoH) converter has been proposed and demonstrated in this paper. Experimental results prove the intended operation and validate the analysis of the converter. This is the first demonstration of a converter achieving a high conversion ratio while providing multiple outputs without a transformer. MiMoH converter extends the application spectrum of switched capacitor-based hybrid converters to a broader range.

ACKNOWLEDGMENT

This work was supported in part by the NSF IUCRC Power Management Integration Center (PMIC), an NSF I/UCRC Award No. 2052809, the PMIC industry members, and the NSF CAREER Award No. 2042525.

REFERENCES

- [1] S. P. Litrán, E. Durán, J. Semião, and C. Díaz-Martín, "Multiple-Output DC-DC Converters: Applications and Solutions," *Electronics*, vol. 11, no. 8, p. 1258, Jan. 2022.
- [2] H.-P. Le, C.-S. Chae, K.-C. Lee, S.-W. Wang, G.-H. Cho, and G.-H. Cho, "A Single-Inductor Switching DC-DC Converter With Five Outputs and Ordered Power-Distributive Control," *IEEE Journal of Solid-State Circuits*, vol. 42, no. 12, pp. 2706–2714, Dec. 2007.
- [3] A. T. Leung Lee, W. Jin, S.-C. Tan, and R. S. Y. Hui, *Single-Inductor Multiple-Output Converters: Topologies, Implementation, and Applications*, 1st ed. Boca Raton: CRC Press, Nov. 2021.
- [4] R.-J. Wai and K.-H. Jheng, "High-Efficiency Single-Input Multiple-Output DC-DC Converter," *IEEE Transactions on Power Electronics*, vol. 28, no. 2, pp. 886–898, Feb. 2013.
- [5] K. Abe, K. Nishijima, K. Harada, T. Nakano, T. Nabeshima, and T. Sato, "A Novel Three-Phase Buck Converter with Bootstrap Driver Circuit," in *2007 IEEE Power Electronics Specialists Conference*, Jun. 2007, pp. 1864–1871.
- [6] P. S. Shenoy, M. Amaro, J. Morroni, and D. Freeman, "Comparison of a Buck Converter and a Series Capacitor Buck Converter for High-Frequency, High-Conversion-Ratio Voltage Regulators," *IEEE Transactions on Power Electronics*, vol. 31, no. 10, pp. 7006–7015, Oct. 2016.
- [7] G.-S. Seo, R. Das, and H.-P. Le, "Dual Inductor Hybrid Converter for Point-of-Load Voltage Regulator Modules," *IEEE Transactions on Industry Applications*, vol. 56, no. 1, pp. 367–377, Jan. 2020.
- [8] R. Das, G.-S. Seo, and H.-P. Le, "Analysis of Dual-Inductor Hybrid Converters for Extreme Conversion Ratios," *IEEE Journal of Emerging and Selected Topics in Power Electronics*, vol. 9, no. 5, pp. 5249–5260, Oct. 2021.
- [15] R. Das and H.-P. Le, "Multi-Output Hybrid Converter and Method Thereof," US Patent US20200212807A1, Jul., 2020.
- [9] T. Xie, R. Das, G. Seo, D. Maksimovic, and H.-P. Le, "Multiphase Control for Robust and Complete Soft-charging Operation of Dual Inductor Hybrid Converter," in *2019 IEEE Applied Power Electronics Conference and Exposition (APEC)*, Mar. 2019, pp. 1–5.
- [10] R. Das and H.-P. Le, "A Regulated 48V-to-1V/100A 90.9%-Efficient Hybrid Converter for POL Applications in Data Centers and Telecommunication Systems," in *2019 IEEE Applied Power Electronics Conference and Exposition (APEC)*, Mar. 2019, pp. 1997–2001.
- [11] R. Das, H.-P. Le, and G. Seo, "Hybrid converter family and methods thereof," US Patent US11152854B2, Oct., 2021.
- [12] Y. Chen, H. Cheng, D. M. Giuliano, and M. Chen, "A 93.7% Efficient 400A 48V-1V Merged-Two-Stage Hybrid Switched-Capacitor Converter with 24V Virtual Intermediate Bus and Coupled Inductors," in *2021 IEEE Applied Power Electronics Conference and Exposition (APEC)*, Jun. 2021, pp. 1308–1315.
- [13] R. Das and H.-P. Le, "A Two-Stage 110VAC-to-1VDC Power Delivery Architecture Using Hybrid Converters for Data Centers and Telecommunication Systems," *Techrxiv Preprints*, DOI: 10.36227/techrxiv.16557711.v1, Sep. 2021.
- [14] Y. Zhu, T. Ge, Z. Ye, and R. C. Pilawa-Podgurski, "A Dickson-Squared Hybrid Switched-Capacitor Converter for Direct 48 V to Point-of-Load Conversion," in *2022 IEEE Applied Power Electronics Conference and Exposition (APEC)*, Mar. 2022, pp. 1272–1278.
- [16] R. Das, J. Celikovic, S. Abedinpour, M. Mercer, D. Maksimovic, and H.-P. Le, "Demystifying Capacitor Voltages and Inductor Currents in Hybrid Converters," in *2019 20th Workshop on Control and Modeling for Power Electronics (COMPEL)*, Jun. 2019, pp. 1–8.
- [17] J. Celikovic, R. Das, H.-P. Le, and D. Maksimovic, "Modeling of Capacitor Voltage Imbalance in Flying Capacitor Multilevel DC-DC Converters," in *2019 20th Workshop on Control and Modeling for Power Electronics (COMPEL)*, Jun. 2019, pp. 1–8.
- [18] R. Das and H.-P. Le, "Gate Driver Circuits With Discrete Components For A GaN-based Multi-Level Multi Inductor Hybrid Converter," *IEEE Transactions on Industrial Electronics*, pp. 1–1, 2022.